Molecular structure, conformational mobility, vibrational spectra, and thermochemistry of peroxyacetic acid: an *ab initio* and density functional study

S. L. Khursan[a]★ *and V. L. Antonovsky*[b] †

[a]*Bashkir State University,*
32 ul. Frunze, 450074 Ufa, Russian Federation.
Fax: +7 (347 2) 22 6105. E-mail: KhursanSL@ufacom.ru
[b]*N. N. Semenov Institute of Chemical Physics, Russian Academy of Sciences,*
4 ul. Kosygina, 119991 Moscow, Russian Federation.
Fax: +7 (095) 938 2156

The structure of the peroxyacetic acid (PAA) molecule and its conformational mobility under rotation about the peroxide bond was studied by *ab initio* and density functional methods. The free rotation is hindered by the *trans*-barrier of height 22.3 kJ mol^{-1}. The equilibrium molecular structure of AcOOH (C_s symmetry) is a result of intramolecular hydrogen bond. The high energy of hydrogen bonding (~46 kJ mol^{-1} according to natural bonding orbital analysis) hampers formation of intermolecular associates of AcOOH in the gas and liquid phases. The standard enthalpies of formation for AcOOH (−353.2 kJ mol^{-1}) and products of radical decomposition of the peroxide — AcO$^{\bullet}$ (−190.2 kJ mol^{-1}) and AcOO$^{\bullet}$ (−153.4 kJ mol^{-1}) — were determined by the G2 and G2(MP2) composite methods. The O—H and O—O bonds in the PAA molecule (bond energies are 417.8 and 202.3 kJ mol^{-1}, respectively) are much stronger than in alkyl hydroperoxide molecules. This provides an explanation for substantial contribution of non-radical channels of the decomposition of peroxyacetic acid. The electron density distribution and gas-phase acidity of PAA were determined. The transition states of the ethylene and cyclohexene epoxidation reactions were located (E_a = 71.7 and 50.9 kJ mol^{-1} respectively).

Key words: peroxyacetic acid, quantum-chemical calculations, *ab initio* quantum-chemical calculations, molecular structure, conformational analysis, vibrational spectra, thermochemistry, acidity, epoxidation.

Peroxy acids, RC(O)OOH, are one of the main classes of organic peroxides. They are widely used as oxidants.[1,2] Reactions of peroxy acids with olefins result in α-oxides (Prilezhaev reaction), which are then transformed into glycols or esters.

Under the action of peroxy acids, carbonyl compounds are converted into esters *via* α-hydroxy peroxy ethers (Bayer—Williger reaction). Peroxy acids oxidize various sulfurous and nitrogen-containing compounds. A remarkable feature of peroxy acids is strong intramolecular hydrogen bond with an energy of 25—30 kJ mol^{-1}.

The structures of organic peroxy acids were experimentally studied by microwave spectroscopy and dielcometry in the gas phase (lower homologs) and by X-ray analysis (higher peroxy acids).[3] In this work we report on the *ab initio* and density functional quantum-chemical calculations of the molecular structure, conformational mobility, vibrational spectra, and thermochemistry of peroxy acids in the free state taking peroxyacetic acid AcOOH (**1**, PAA) as an example, because experimental studies were mainly carried out in the condensed state while gas-phase studies of peroxy acids are complicated by their thermal instability.

Calculation Procedure

The *ab initio* and density functional (DFT) quantum-chemical calculations were carried out using the GAMESS[4] and GAUSSIAN-98[5] programs. *Ab initio* calculations were carried out by the restricted Hartree—Fock method, RHF (for radicals, the unrestricted Hartree—Fock approximation, UHF, was employed), while the DFT calculations were performed using the B3LYP hybrid functional.[6] The RHF calculations were carried out with inclusion of electron correlation effects at the second and fourth order levels of Møller—Plesset perturbation theory (MP2 and MP4, respectively). All calculations of the molecular geometry and conformational mobility and the vibrational spec-

† Deceased.

Published in Russian in *Izvestiya Akademii Nauk. Seriya Khimicheskaya,* No. 9, pp. 1809—1819, September, 2003.

1066-5285/03/5209-1908 $25.00

trum of **1** were performed with the 6-31G(d,p) basis set (the 6-31G split valence basis set augmented with polarization d-functions for the non-hydrogen atoms and p-functions for H atoms). Intermolecular association of PAA was studied using the 6-311++G(d,p) extended basis set.

The ground-state geometries of the molecules of the compounds under study were determined by full geometry optimization. The potential curves of internal rotation about the peroxide bond were obtained by calculations with the constant value of the dihedral, or torsion, angle φ, which characterizes the mutual arrangement of the atoms in the C—O—O—H fragment, and full optimization of the remaining geometric parameters. These calculations were carried out with a φ increment of 10° in the range 0—180° with allowance for symmetry considerations.

The relative energies of conformers were calculated as the total energy differences between the given state and the ground state of the peroxide molecule. In performing MP2 optimizations the relative energies of different molecular states were also estimated at the MP4 level with inclusion of the single, double, and quadruple excitations (MP4-SDQ) by carrying out single-point calculations with fixed geometric parameters in the same basis set. MPn optimizations were carried in the "frozen core" approximation.

Calculations of the ground states of the molecules under study included the solution to the vibrational problem and determination of the force constants, vibrational frequencies (ν), and zero-point vibrational energy corrections (ZPE). In comparing the results of calculations with the published data, the calculated ν and ZPE values were corrected by multiplying them by the corresponding scale factor.[7]

To interpret structural peculiarities of the PAA molecule using the bonding orbital populations and the molecule-stabilizing orbital effects, the natural bonding orbital (NBO) approach[8] was employed in the framework of the B3LYP/6-31G(d,p) approximation.

The enthalpies of formation of PAA and products of its decomposition were calculated using the isodesmic approach.[9] The enthalpies of the compounds and radicals involved in the isodesmic reactions were calculated in the MP4//MP2/6-31G(d,p) and B3LYP/6-31G(d,p) approximations and using two composite computational schemes, G2[10] and G2(MP2).[11]

Results and Discussion

Molecular structure of PAA. Calculations with full optimization of the molecular geometry of PAA gave the equilibrium structure with C_s symmetry. The main geometric parameters (bond lengths and bond angles) in the AcOOH molecule are shown in Fig. 1, *a* and listed in Table 1 (for comparison, here we also present the experimental data on the structure of the peroxide fragment). The results obtained by the main computational methods are in good agreement, while extension of the basis set has little effect on the calculated values of geometric parameters. For clarity from this point on we will use the results obtained from B3LYP/6-31G(d,p) calculations. The peroxide bond length in the PAA molecule (r = 1.442 Å) is

Table 1. Geometric parameters and energy characteristics of the equilibrium structure of the peroxyacetic acid molecule calculated using different methods in the 6-31G(d,p) and 6-311++G(d,p) basis sets

Parameter	6-31G(d,p)			6-311++G(d,p)		Experiment*
	RHF	MP4//MP2	B3LYP	MP2	B3LYP	
Bond			*r*/Å			
C(1)—O(2)	1.3275	1.3598	1.3541	1.3569	1.3547	1.33
O(2)—O(3)	1.3884	1.4561	1.4422	1.4372	1.4392	1.47
O(3)—H(9)	0.9553	0.9849	0.9886	0.9813	0.9841	1.0
C(1)=O(4)	1.1898	1.2209	1.2155	1.2120	1.2088	1.22
C(1)—C(5)	1.4997	1.4982	1.5026	1.4994	1.5000	—
O(4)...H(9)	1.9266	1.8524	1.8516	1.8673	1.8886	—
Bond angle			θ/deg			
C(1)—O(2)—O(3)	113.1	110.2	110.9	110.8	111.6	112.9
O(2)—O(3)—H(9)	103.3	99.4	99.7	100.4	101.0	96.0
O(4)=C(1)—O(2)	122.1	122.5	121.9	122.3	121.8	—
O(4)=C(1)—C(5)	126.0	127.1	127.0	127.3	127.2	—
C(1)=O(4)...H(9)	83.6	83.9	84.3	84.0	84.7	—
O(4)...H(9)—O(3)	117.9	124.1	123.2	122.6	121.0	—
Torsion angle			φ/deg			
C(1)—O(2)—O(3)—H(9)	0.0	0.0	0.0	0.0	0.0	—
O(4)=C(1)—O(2)—O(3)	0.0	0.0	0.0	0.0	0.0	—
μ/D	2.28	2.60	2.34	2.67	2.50	—
E_{tot}/hartree	−302.571638	−303.415411	−304.217686	−303.555569	−304.312075	—
ΔE_{trans}/kJ mol^{-1}	16.0	17.6	22.3	—	—	—
ZPE/kJ mol^{-1}	185.0	174.7	171.0	171.4	169.7	—

* Data taken from Ref. 3.

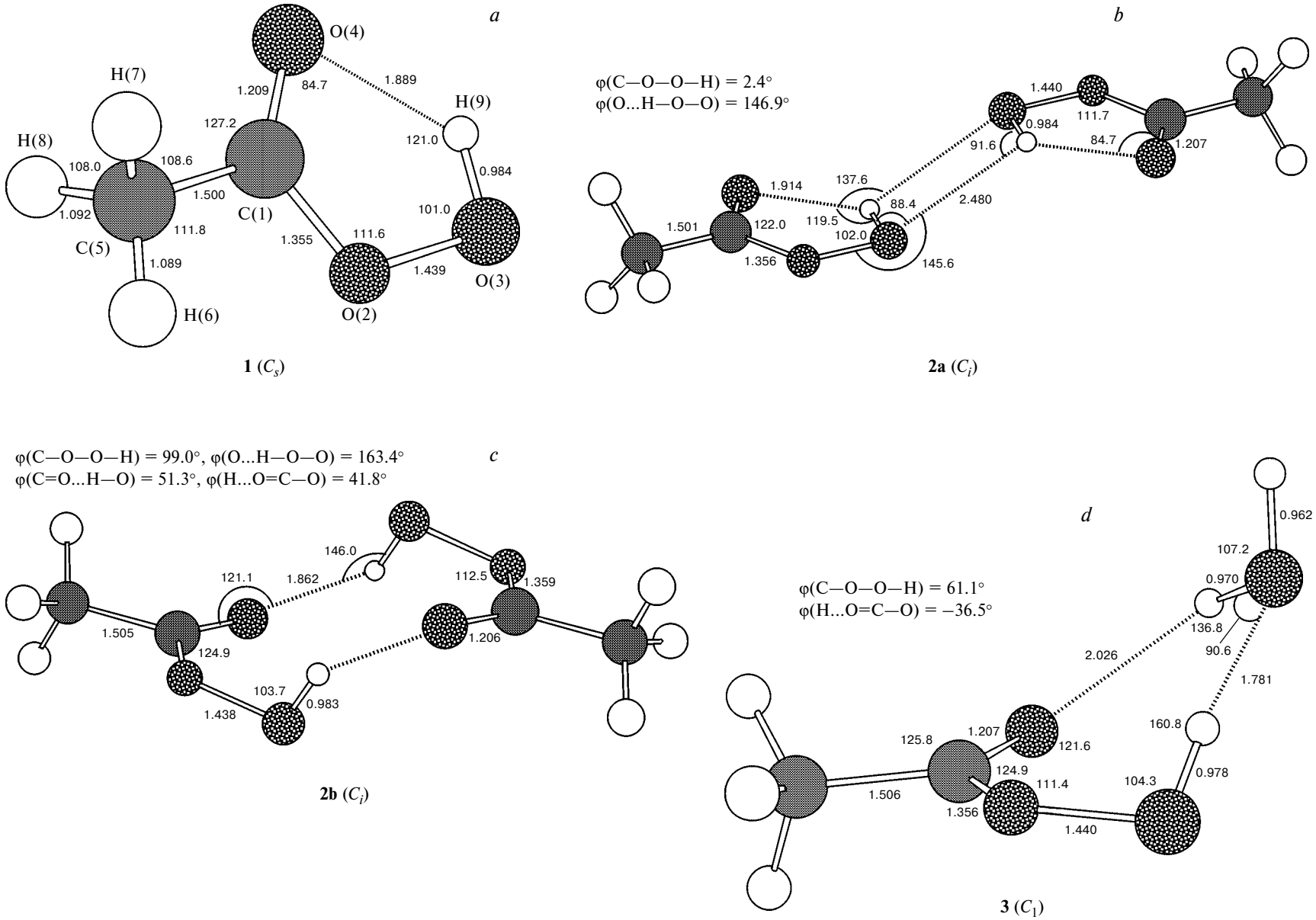

Fig. 1. Molecular structures of peroxyacetic acid (**1**) (*a*), its dimers **2a** (*b*) and **2b** (*c*), and complex $AcOOH \cdot H_2O$ (**3**) (*d*) obtained from B3LYP/6-311++G(d,p) calculations. The interatomic distances are given in Å and the bond angles are given in degrees. The symmetries of the structures are given in parentheses.

typical of peroxide compounds, whereas the C—O bond is much shorter than in the alkylperoxide molecules, namely, 1.354 Å *vs.* 1.417 Å in MeOOH.[12] The reason for the decrease in *r*(C—O) is clear; this is the effect of the carbonyl group. The orbital interactions, which describe this effect, are considered below. The O—O—H bond angle (99.7°) is close to that in hydroperoxides (99.8° for MeOOH molecule), whereas the C—O—O angle is somewhat larger (110.9° and 106.1°, respectively), which is also associated with the effect of the carbonyl oxygen atom. The most remarkable feature of the molecular structure of AcOOH, which strongly differs peroxy acids from alkylhydroperoxides ROOH, is the magnitude of the C—O—O—H torsion angle (φ). If alkylhydroperoxides adopt a *gauche*-conformation (φ ≈ 90—110° depending on the nature of R), the AcOOH molecule is characterized by φ = 0, which corresponds to planar arrangement of the atoms in the carboperoxyl fragment. The results obtained confirm that peroxy acids are compounds with strong intramolecular hydrogen bond (IHB). The equilibrium distance between the atoms participating in the hydrogen bond is 1.852 Å while the C=O...H and O...H—O angles are 84.3 and 123.2°, respectively. In the gas phase and even in the liquid phase, peroxy acids exist almost without exception in the monomeric form.[2] In the solid state, they undergo dimerization[13] (the proposed structure of the dimer is shown below).

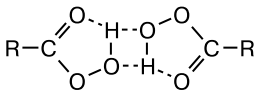

We calculated intermolecular complexes of PAA taking its dimers and the AcOOH · H_2O complex as examples. The calculations were carried out in the B3LYP/6-31G(d,p) approximation. Then, the equilibrium structure of the complex was refined by the B3LYP/6-311++G(d,p) method. The results of energy calculations for various tentative structures of the complexes clearly indicate that the roles of hydrogen bond acceptor and donor in the PAA molecule are played by the H atom of the hydroperoxide group and the carbonyl O atom, respectively. Interactions with O atoms of the peroxy group are much weaker or do not manifest themselves at all.

In calculating the AcOOH dimers we located two structures (**2a,b**) belonging to the C_i point symmetry group (see Fig. 1, *b*, *c*). Complex **2a** proposed by Swern[13] is energetically less favorable ($\Delta H^\circ = -3.8$ kJ mol^{-1}), because the hydrogen bond is formed involving the O_β atom of the peroxy group. The intermolecular H-bond is rather long (2.480 Å). The molecular structure of PAA in complex **2a** remains virtually unchanged as compared to the AcOOH monomer. Complex **2b** is somewhat stronger ($\Delta H^\circ = -16.1$ kJ mol^{-1}), because the H-bond is formed involving the carbonyl O atom. Here, the length of the intermolecular H-bond is 1.862 Å. Nonplanar structure of the C(O)OOH fragment (φ = 99.0°) is a structure-destabilizing factor.

The equilibrium structure of the complex AcOOH · H_2O (**3**) is shown in Fig. 1, *d*. Both molecules simultaneously act as the hydrogen bond donor and acceptor. The shorter H_2O...H bond is somewhat stronger, the O...H—O angle (160.8°) is close to 180°, which is typical of strong hydrogen bonds. The torsion angle φ in complex **3** is 61.1°; other geometric parameters vary only slightly compared to those of the free PAA molecule. The change in the enthalpy upon the formation of complex **3** (−16.8 kJ mol^{-1}) is fully compensated by the low entropy of its formation (−126.4 J mol^{-1} K^{-1}), so that the change in the Gibbs free energy at 298 K is positive (ΔG° = 20.9 kJ mol^{-1}). Calculations of normal vibrational frequencies of all the associates studied in this work revealed the absence of imaginary frequencies, which permitted the structures located to be identified as stable intermolecular complexes.

Efficient dimerization of PAA is precluded by low entropy of complexation (−127.7 and −137.4 J mol^{-1} K^{-1} for **2a** and **2b**, respectively). Thus, the results of quantum-chemical calculations confirm the conclusions drawn earlier[2] that PAA mainly exists in the monomeric form even in the liquid phase.

According to the results of an X-ray study of solid peroxy acids $C_nH_{2n+1}C(O)OOH$ (n = 9—16),[13] the effective size of their dimers (in Å) can be evaluated using the relationship 3.307 + 2.126n, where n is the number of C atoms in the peroxy acid molecule. Hence, the most distant C atoms of the Me groups in the AcOOH molecule are separated by 7.56 Å, which is in good agreement with the available data for dimer **2b**: *r*(Me...Me) = 7.70 Å. For structure **2a**, this distance is much longer (*r* = 9.44 Å). These results, as well as the energy characteristics, suggest that the most probable structure of solid AcOOH is dimer **2b**, which undergoes irreversible dissociation on going to the liquid or gaseous state.

Vibrational spectrum. Table 2 lists the calculated and experimental[14] vibrational spectra of PAA. The main difference of these spectra from those of alkylperoxides studied earlier[15] is considerable mixing of the vibrations of the peroxide bond with the vibrations of adjacent bonds.

The Raman lines corresponding to the stretching vibration of the O—O bond in peroxide molecules are known to be strong.[16] In the PAA molecule, this vibration is less characteristic and localized as compared to the hydroperoxide molecules. Namely, calculations of the potential energy distribution estimate the ν(OO) contribution at 44% (*cf.* more than 60% for alkylperoxides[15]). This vibration is mixed with the C—C (21%) and C—O (24%) stretching vibrations and manifests itself in the IR (Raman) spectra of peroxy acids as a band (line) of medium intensity.

Table 2. Experimental and calculated vibrational spectra of peroxyacetic acid

Calculations[a]					Experiment[14]				
ν/cm^{-1}	I_{IR}[b]	I_{Raman}[c]	ρ	PED	ν_{IR}/cm^{-1}	I[d]	ν_{Raman}/cm^{-1}	I[e]	ρ
86	0.01	0.12	0.75	96τ(CC)	219	—	224	2	dp
207	0.00	0.29	0.75	82τ(CO)	—	m	139	1	dp
302	0.38	0.33	0.20	51δ(CCO), 36δ(COO)	325	s	323	10	0.3
402	2.03	3.28	0.75	97τ(OO)	450	s	—	30	0.3
410	0.28	1.25	0.36	35δ(CCO), 25δ(COO), 22δ(OCO)	425	w	432	—	—
584	0.85	0.29	0.75	78τ(O=COO)	618	s	610	sh	dp
619	0.26	6.96	0.36	39δ(OCO), 35ν(CC)	648	m	640	80	0.2
832	0.80	4.76	0.14	38ν(OO), 42ν(CO), 15δ(COO)	866	m	860	12	0.6
924	0.06	2.17	0.67	44ν(OO), 24ν(CO), 21ν(CC)	940	s	936	60	0.15
990	0.13	6.07	0.24	55δ(CCH), 13ν(CC), 10τ(CC)	1010	vw	1004	40	0.1
1020	0.21	0.37	0.75	64δ(CCH), 19τ(CC), 10τ(O=COO)	1040	m	—	—	—
1223	4.65	1.49	0.45	39ν(CO), 18ν(CC), 17δ(OCO)	1233	s	1225	3	0.66
1360	0.42	2.77	0.75	85δ(CCH)	1369	m	1370	3	0.7
1404	3.67	7.39	0.71	94δ(OOH)	1439	—	1438	2	dp
1436	0.19	13.27	0.75	79τ(CC), 21δ(CCH)	—	m	1410	—	—
1443	0.30	11.52	0.75	72τ(CC), 24δ(CCH)	1429	s	—	6	dp
1720	3.93	9.90	0.20	82ν(C=O)	1750	m	1750	20	0.2
2955	0.00	108.3	0.00	100ν(CH)	2940	—	2945	—	—
3042	0.02	59.97	0.75	100ν(CH)	2990	w	2988	150	p
3084	0.04	46.50	0.75	100ν(CH)	—	w	—	40	dp
3323	1.52	22.79	0.13	100ν(OH)	3340	s	—	—	—

Note. PED is potential energy distribution and ρ is the depolarization degree.
[a] This work; obtained from MP2/6-31G(d,p) calculations.
[b] IR intensity/D^2 a.m.u.$^{-1}$ Å^{-2}.
[c] Raman intensity/Å^4 a.m.u.$^{-1}$.
[d] Experimental intensity/rel. units.

The bands (lines) characteristic of peroxy acids are as follows: ν(OH) (3370), ν(C=O) (1750), ν(OO) (870), ρ(C=O) (600), and δ(COO) (330 cm^{-1}).[2] The results of our calculations are by and large in agreement with these values: the corresponding vibrational frequencies for the AcOOH molecule are 3323 (3340), 1720 (1750), 924 (940), 584 (618), and 302 (325) cm^{-1}. Here, figures in parentheses are the experimental data.

A comparison of the results of calculations and experimental data (see Table 2) points to high reliability of theoretical estimates of the vibrational frequencies of peroxide compounds, which allows the intense IR band at 1404 cm^{-1} corresponding to the deformation vibration of the O—O—H angle to be recommended for determination of the concentration of PAA in solution. The IR monitoring of AcOOH is favored by the low ability of PAA to form intermolecular associates (see above). At the same time, the δ(OOH) vibration in the IR spectra of higher peroxy acids can be masked by intense bending vibrations of C—H bonds.

Thermochemistry of peroxyacetic acid and products of its decomposition. Taking into account the small size of the AcOOH molecule, the enthalpies of formation of PAA and radical products of its decomposition can be estimated using composite computational methods G2 and G2(MP2),[10,11] which provide a high accuracy of calculations. To demonstrate the potentialities of these methods, we calculated the enthalpies of formation ($\Delta_f H^\circ_{298}$) of AcOOH and some related compounds using the following relationship

$$\Delta_f H^\circ_{298}(C_xH_yO_z) = x\Phi(C) + y\Phi(H) + z\Phi(O) + H^\circ_{298}(C_xH_yO_z), \quad (1)$$

where Φ are the enthalpy functions of the corresponding atoms (differences between the experimental standard enthalpy of formation of an atom and the enthalpy of the same atom obtained from G2 or G2(MP2) calculations) and $H^\circ_{298}(C_xH_yO_z)$ is the enthalpy of the compound under study, calculated using the G2 or G2(MP2) procedure. The results of $\Delta_f H^\circ_{298}$ calculations are listed in Table 3. The mean error of calculations is about 3 kJ mol^{-1} for the G2 procedure and nearly twice as large for the G2(MP2) method, which somewhat underestimates the $\Delta_f H^\circ_{298}$ values.

The remaining error of calculations seems to be systematic and can be included using, *e.g.*, the isodesmic

Table 3. Enthalpies of formation ($\Delta_f H^\circ_{298}$/kJ mol^{-1}) and enthalpies (H°_{298}/hartree) of various peroxides and related compounds calculated by the G2 or G2(MP2) methods

Compound	G2		G2(MP2)		$\Delta_f H^\circ_{298}$*
	$\Delta_f H^\circ_{298}$	H°_{298}	$\Delta_f H^\circ_{298}$	H°_{298}	
HO$^\bullet$	38.4	−75.640603	37.5	−75.637619	39.3
H_2O	−242.5	−76.328277	−245.9	−76.326233	−241.8
HOO$^\bullet$	15.0	−150.724117	10.9	−150.718973	14.6
HOOH	−134.2	−151.361600	−140.1	−151.357145	−136.1
MeO$^\bullet$	20.8	−114.863562	21.6	−114.859521	17.2
MeOH	−205.9	−115.530607	−207.7	−115.527527	−201.7
MeOO$^\bullet$	10.5	−189.942080	7.5	−189.936101	18.8
MeOOH	−132.2	−190.577107	−137.0	−190.571794	−131.0
AcO$^\bullet$	−191.0	−228.073707	−193.2	−228.067025	—
AcOH	−437.5	−288.748274	−440.9	−228.742055	−432.2
AcOO$^\bullet$	−160.2	−303.136555	−164.6	−303.127367	—
AcOOH**	−355.5	−303.791627	−362.0	−303.783199	—

* Data taken from Ref. 17.

** The zero-point vibrational energies were calculated by the B3LYP/6-31G(d,p) method because the HF/6-31G(d) approximation employed in the G2 and G2(MP2) procedures gives one negative vibrational frequency for the ground state of the AcOOH molecule.

approach. For instance, the following two isodesmic reactions (IDR) were constructed for acetic acid

$$AcOH + HCHO \longrightarrow MeCHO + HCOOH, \quad (2)$$

$$AcOH + 2\,CH_4 \longrightarrow C_2H_6 + MeOH + HCHO. \quad (3)$$

The calculated thermal effects of these reactions and the corresponding experimental data are listed in Table 4. A comparison shows that the isodesmic approach permits good agreement between theory and experiment, especially when using the G2 computational procedure. The results obtained by the MP2 and B3LYP methods are somewhat worse.

Thus, the joint use of the isodesmic approach and calculations by the composite methods G2 and G2(MP2) allows reliable determination of the enthalpies of formation and energies of chemical bonds in the molecules of PAA and related compounds.

To this end, we constructed some IDR for AcOOH (Eqs. (4) and (5)), AcO$^\bullet$ (Eqs. (6) and (7)), and AcOO$^\bullet$ (Eqs. (8) and (9)).

$$AcOOH + H_2O \longrightarrow AcOH + HOOH \quad (4)$$

$$AcOOH + MeOH \longrightarrow AcOH + MeOOH \quad (5)$$

$$AcO^\bullet + H_2O \longrightarrow AcOH + HO^\bullet \quad (6)$$

$$AcO^\bullet + MeOH \longrightarrow AcOH + MeO^\bullet \quad (7)$$

$$AcOO^\bullet + HOOH \longrightarrow AcOOH + HOO^\bullet \quad (8)$$

$$AcOO^\bullet + MeOOH \longrightarrow AcOOH + MeOO^\bullet \quad (9)$$

Using the G2 and G2(MP2) methods, we determined the thermal effects of the reactions (4)—(9). Then, the enthalpies of formation for PAA (reactions (4) and (5)) and for acetyloxy (reactions (6) and (7)), and acetylperoxy radicals (reactions (8) and (9)) were calculated using the known experimental $\Delta_f H^\circ_{298}$ values for the compounds involved in the IDR (see Table 3). The results obtained are presented in Table 5.

Table 4. Thermal effects (kJ mol^{-1}) of isodesmic reactions constructed for acetic acid

Computational method	Reaction (2)	Reaction (3)
MP2/6-31G(d,p)	−5.8	193.0
B3LYP/6-31G(d,p)	−9.6	192.2
G2(MP2)	−2.3	183.1
G2	−2.4	185.2
Ref. data[17]	−3.4	186.6

A comparison of the data for AcOOH, AcO$^\bullet$, and AcOO$^\bullet$ (see Tables 3 and 5) demonstrates reproducibility of the $\Delta_f H^\circ_{298}$ values. Based on the results obtained, we determined the dissociation energies (D) of the O—O and O—H bonds in the PAA molecule. These are D(AcOO—H) = 417.8 kJ mol^{-1} and D(AcO—OH) = 202.3 kJ mol^{-1}, which is appreciably higher than the corresponding values for alkylhydroperoxides. The strength of the O—O bond approaches the value known for hydrogen peroxide molecule. This provides an explanation for substantial contribution of non-radical channels of the decomposition of AcOOH.[18,19] It is appropriate to remind that the D value corresponds to the energy change in the case of homolytic dissociation of the O—O bond after the molecular fragments moved apart to infinity. Real homolytic reactions are complicated by homo- and heteromolecular association of AcOOH and products of its decomposition, which is responsible for significant difference between the activation energies of homolysis of peroxy acids (125—142 kJ mol^{-1}) and the peroxide bond strength calculated here.

Table 5. Thermal effects of reactions (kJ mol^{-1}) and enthalpies of formation ($\Delta_f H°_{298}$/kJ mol^{-1}) of peroxyacetic acid and acetyloxy and acetylperoxy radicals obtained from G2 and G2(MP2) calculations

Compound	Thermal effect				$\Delta_f H°_{298}$				
	Reaction (4), (6), (8)		Reaction (5), (7), (9)		Reaction (4), (6), (8)		Reaction (5), (7), (9)		Average value
	G2	G2(MP2)	G2	G2(MP2)	G2	G2(MP2)	G2	G2(MP2)	
AcOOH	26.3	26.9	−8.3	−8.2	−352.8	−353.4	−353.2	−353.3	−353.2
AcO$^{\bullet}$	34.4	35.7	−19.7	−18.4	−185.5	−186.8	−193.6	−194.9	−190.2
AcOO$^{\bullet}$	−46.2	−46.4	−52.6	−52.9	−156.3	−156.1	−150.8	−150.5	−153.4

Conformational mobility. The molecular structure of peroxyacetic acid permits rotation about three axes (C(1)—C(5), C(1)—O(2), and O(2)—O(3) bonds, see Fig. 1); however, only rotation about the last-named bond is significant for realization of different conformations of the peroxide fragment. Rotation about the C—O bond is essentially hindered by strong orbital interactions in the molecule (see below); therefore, in all the conformations studied the C(5), C(1), O(4), O(2), and O(3) atoms can be treated as lying in nearly the same plane. High barrier to rotation about the C—O bond was also reported for acetylperoxy nitrate.[20,21]

Variation of the energy of the AcOOH molecule upon rotation about the O—O bond is shown in Fig. 2. In contrast to other classes of peroxide compounds, which have two reflection symmetric stable states, in this case the potential curve has one minimum at φ = 0° corresponding to the *cis*-structure of the AcOOH molecule and one maximum at φ = 180° corresponding to the *trans*-barrier. According to B3LYP/6-31G(d,p) calculations, ΔE_{trans} = 22.3 kJ mol^{-1}, which is much higher than the *trans*-barriers for alkylperoxides and alkylhydroperoxides, peroxy esters and diacylperoxides (ΔE_{trans} = 0.1—8.1 kJ mol^{-1}).[12] The *cis*-conformations of these molecules correspond to the most unstable structures; however, the energy of the strong IHB in the AcOOH molecule is much higher than the *cis*-barrier.

Rotation of hydroxyl group about the O—O bond is accompanied by regular variations of the geometric parameters of the peroxide fragment. Figures 3 and 4 present the dependences of the O—O and C—O bond lengths and the C—O—O (θ) and O—O—H (ψ) bond angles on the

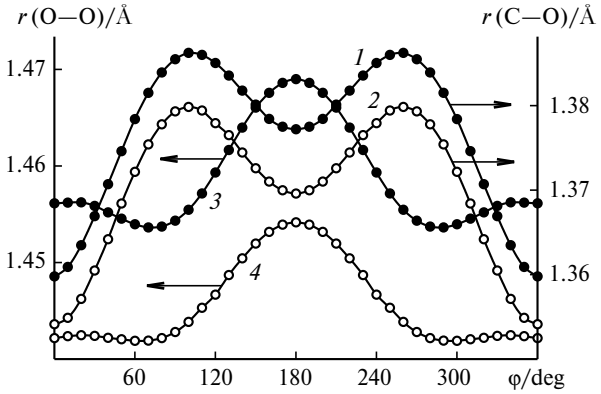

Fig. 3. Variation of the C—O (*1*, *2*) and O—O (*3*, *4*) bond lengths upon internal rotation about the O—O bond in the peroxyacetic acid molecule according to MP2 (*1*, *3*) and B3LYP (*2*, *4*) calculations.

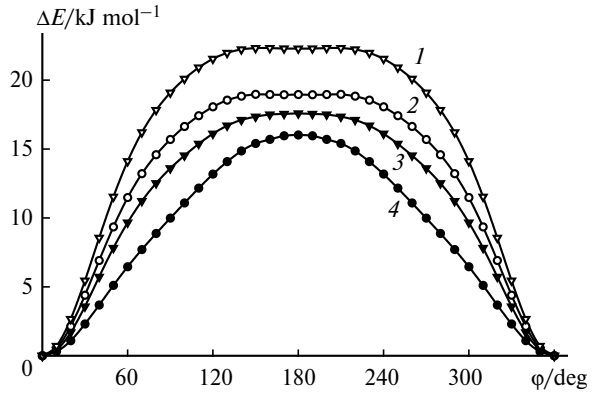

Fig. 2. Potential curves of internal rotation about the O—O bond in the peroxyacetic acid molecule, obtained from B3LYP (*1*), MP2 (*2*), MP4//MP2 (*3*), and RHF calculations (*4*) in the 6-31G(d,p) basis set.

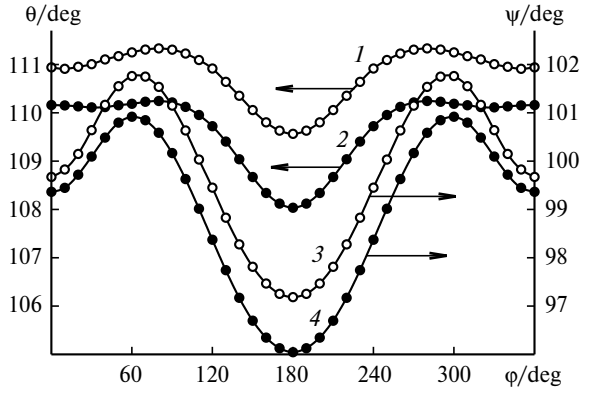

Fig. 4. Variation of the C—O—O (θ) (*1*, *2*) and O—O—H (ψ) (*3*, *4*) bond angles upon internal rotation about the O—O bond in the peroxyacetic acid molecule according to B3LYP (*1*, *3*) and MP2 (*2*, *4*) calculations.

torsion angle φ. The interval $-60° < \varphi < 60°$ corresponds to manifestation of the IHB, which "stretches" the peroxide fragment of the AcOOH molecule, thus resulting in relative decrease in both the bond lengths and bond angles. Beyond this range, the patterns of the changes in the geometric parameters of the peroxide fragment are identical to the patterns found for alkylperoxides and alkylhydroperoxides[12] (monotonic changes in bond angles with minima at 180° and the presence of a minimum (maximum) for the O—O (C—O) bond length at $\varphi \approx \pm 80°$).

These regularities of the changes in the molecular structure of AcOOH are due to a complex pattern of structure-stabilizing orbital interactions. The predominant electronic effects and their energy characteristics were studied using the NBO approach.[8] The most important orbital interactions and their energies at different φ values are listed in Table 6. These electronic effects can be divided into three groups.

The first group comprises the interactions, which describe the hydrogen bond. The overlap of the lone electron pairs (LEP) of the carbonyl O atom and the antibonding orbital of the O—H bond provides a considerable energy gain (45.9 kJ mol^{-1} for the equilibrium structure of the PAA molecule) and a full suppression of the *cis*-barrier. Two LEPs of the O atom are represented by the nonbonding π- and σ-orbitals and the largest contribution to the hydrogen bond comes from the $n_\pi(O(4)) \rightarrow \sigma^*(O(3)—H(9))$ interaction. The orbital overlap energy monotonically decreases as φ increases and becomes infinitesimally small (less than the threshold value, 2 kJ mol^{-1}) at $\varphi = 60°$. Indeed, the O(4)—H(9) distance in the conformer with $\varphi = 60°$ becomes longer than the sum of the van der Waals radii of oxygen and hydrogen.

The second group comprises the interactions involving the anomeric effect. The interaction between the LEPs and the vacant orbitals of adjacent polar bonds, which stabilizes the *gauche*-conformation of organic molecule, is basic to the anomeric effect.[22] It is known[12,15] that the $n_\pi \rightarrow \sigma^*(C—O)$ and $n_\pi \rightarrow \sigma^*(O—H)$ interactions stabilize various peroxide molecules. The PAA molecule is also no exception (see Table 6). However, the energy of the IHB

Table 6. Energies of orbital interactions in peroxyacetic acid molecule, calculated using the NBO approach at different values of the torsion angle (φ)

Interaction	Energies of orbital interactions (kJ mol^{-1}) at φ/deg									
	0	10	20	30	40	50	60	70	80	
$n_\sigma(O(3)) \rightarrow \sigma^*(C(1)—O(2))$	14.2	14.0	13.4	11.9	9.0	5.8	3.8	2.8	2.2	
$n_\sigma(O(2)) \rightarrow \sigma^*(O(3)—H(9))$	7.4	7.3	7.0	6.6	5.9	5.1	4.2	3.3	2.5	
$n_\pi(O(3)) \rightarrow \sigma^*(C(1)—O(2))$	—	—	—	3.3	7.7	11.8	13.7	14.2	14.1	
$n_\pi(O(2)) \rightarrow \sigma^*(O(3)—H(9))$	—	—	—	—	—	—	3.6	4.2	4.5	
$n_\sigma(O(2)) \rightarrow \sigma^*(C(1)=O(4))$	22.6	22.3	21.5	21.2	21.1	21.2	21.4	21.7	22.0	
$n_\pi(O(2)) \rightarrow \pi^*(C(1)=O(4))$	207.4	197.2	179.0	169.7	164.5	161.2	159.5	158.4	156.9	
$n_\sigma(O(4)) \rightarrow \sigma^*(O(3)—H(9))$	9.1	8.4	6.5	4.2	2.3	—	—	—	—	
$n_\sigma(O(4)) \rightarrow \sigma^*(C(1)—O(2))$	9.5	9.2	8.5	7.5	6.7	6.1	5.8	5.7	5.7	
$n_\sigma(O(4)) \rightarrow \sigma^*(C(1)—C(5))$	7.7	7.9	8.6	9.5	10.5	11.3	11.8	12.2	12.4	
$n_\pi(O(4)) \rightarrow \sigma^*(C(1)—O(2))$	132.6	134.1	138.2	143.9	149.7	155.5	160.2	163.9	166.7	
$n_\pi(O(4)) \rightarrow \sigma^*(C(1)—C(5))$	75.4	75.6	75.9	76.4	76.7	77.3	77.9	78.4	78.8	
$n_\pi(O(4)) \rightarrow \sigma^*(O(3)—H(9))$	36.8	33.7	26.0	17.0	9.5	4.4	—	—	—	
	φ/deg									
	90	100	110	120	130	140	150	160	170	180
$n_\sigma(O(3)) \rightarrow \sigma^*(C(1)—O(2))$	—	—	—	—	—	—	—	—	—	—
$n_\sigma(O(2)) \rightarrow \sigma^*(O(3)—H(9))$	—	—	—	—	—	—	—	—	—	—
$n_\pi(O(3)) \rightarrow \sigma^*(C(1)—O(2))$	13.3	9.2	10.8	8.6	6.5	4.5	2.6	—	—	—
$n_\pi(O(2)) \rightarrow \sigma^*(O(3)—H(9))$	4.5	4.1	3.5	2.7	—	—	—	—	—	—
$n_\sigma(O(2)) \rightarrow \sigma^*(C(1)=O(4))$	22.2	22.3	22.5	22.6	22.5	22.4	22.3	22.3	22.2	22.3
$n_\pi(O(2)) \rightarrow \pi^*(C(1)=O(4))$	155.7	155.0	155.5	157.1	158.7	161.3	164.3	167.5	170.3	173.5
$n_\sigma(O(4)) \rightarrow \sigma^*(O(3)—H(9))$	—	—	—	—	—	—	—	—	—	—
$n_\sigma(O(4)) \rightarrow \sigma^*(C(1)—O(2))$	5.8	5.9	6.0	6.1	6.1	6.2	6.2	6.2	6.2	6.2
$n_\sigma(O(4)) \rightarrow \sigma^*(C(1)—C(5))$	12.5	12.6	12.6	12.6	12.6	12.5	12.5	12.4	12.4	12.4
$n_\pi(O(4)) \rightarrow \sigma^*(C(1)—O(2))$	168.7	170.0	170.7	170.6	170.5	169.9	169.3	168.7	168.2	168.1
$n_\pi(O(4)) \rightarrow \sigma^*(C(1)—C(5))$	79.2	79.5	79.8	79.9	80.2	80.3	80.5	80.5	80.6	80.7
$n_\pi(O(4)) \rightarrow \sigma^*(O(3)—H(9))$	—	—	—	—	—	—	—	—	—	—

is higher than the energy of these interactions; therefore, the anomeric effect manifests itself only as shortening of the peroxide bond and lengthening of the C—O bond at φ values, which correspond to the maximum energies of the $n_\pi \rightarrow \sigma^*$ interactions. Other nonbonding orbitals (n_σ) of O atoms of the peroxide bridge can be overlapped with the σ*-orbitals of the C—O and O—H bonds at small φ values. These interactions act in line with the hydrogen bonding and decrease the energy of the stable *cis*-conformer, thus increasing the *trans*-barrier.

The third group of interactions is responsible for stabilization of the carboperoxyl fragment. Here, we deal with the following orbital interactions: the overlap of both LEPs of the O(4) atom with the antibonding σ*-orbitals of the C(1)—O(2) and C(1)—C(5) bonds and the $n_\pi(O(2)) \rightarrow \pi^*(C(1)=O(4))$ and $n_\sigma(O(2)) \rightarrow \sigma^*(C(1)=O(4))$ interactions (see Table 6). Their energies are virtually independent of the angle φ. These interactions are the strongest ones in the AcOOH molecule. They stabilize the carboperoxyl fragment and restrict its conformational mobility. For instance, the $n_\pi(O^*(2)) \rightarrow \pi^*(C(1)=O(4))$ overlap produces steric hindrances to free rotation about the C—O bond and is responsible for planarity of the C(5)—C(1)(O(4))—O(2)—O(3) fragment in all the conformations of the AcOOH molecule studied in this work (the maximum deviation from planar structure is 12.6°). Stabilization of the carboperoxyl fragment causes shortening of the C(1)—C(5), C(1)=O(4), and C(1)—O(2) bonds, the last-named bond being affected to the greatest extent.

Electron density distribution and acidic properties. The electron density distribution (in units of electron charge; population analysis according to Mulliken) in the PAA molecule points to significant molecular polarization. A comparison of the effective atomic charges of oxygens in the peroxide bridges (Table 7) in various hydroperoxides shows that a decrease in the electron density on the O atoms correlates with the increase in the strength of the O—O bond. NBO analysis revealed that the presence of electron-acceptor substituents R (MeC(O), CF_3) in the hydroperoxide molecule, ROOH, causes an increase in the energy of the $n(O(3)) \rightarrow \sigma^*(R—O(2))$ interaction and in the extent of the LEP delocalization into an antibonding orbital. On the one hand, this leads to a decrease in the electron density on the O atom. On the other hand, it also causes weakening of repulsion the between the LEPs and an increase in *D*(O—O).

Yet another important factor responsible for the strength of the peroxide bond is stability of the newly formed radical RO$^\bullet$. It seems likely that stabilization of the acetoxy radical due to delocalization of the unpaired electron over the carboxylic fragment is responsible for the decrease in *D*(O—O) compared to trifluoromethylhydroperoxide (see Table 7).

One can assume that the acidity of MeC(O)OH and other hydroperoxides depends on the degree of polarization of the O—H bond. The data in Table 8 show that, in spite of monotonic change in the acidic properties of compounds ROH, ROOH, and ROOOH with an increase in the effective atomic charge of H, the polarity of the O—H bond is not the main factor. The only, but remarkable, exception is acetic acid. Indeed, the acidic properties are governed by the ease of proton abstraction in the reaction

$$RO_xH \rightleftharpoons RO_x^- + H^+,$$

i.e., by the relative stability of the compound and its deprotonated form. In solution, this equilibrium is strongly affected by the solvation of the molecule and anion.

Correlation with the acidic properties of the O—H bond is expected to be more natural if we take the total energy difference between the anion and molecule (*i.e.*, gas-phase acidity) as the reactivity index. The data in Table 8 exhibit a satisfactory correlation between the ΔE_{tot} and pK_a values for compounds ROH and ROOH. Unfortunately, it is impossible to supplement this series with hydrotrioxides, because the hydrotrioxide anion is unstable and barrierlessly decomposes into RO^- and dioxygen molecule.[23]

Table 7. Effective atomic charges (*q*/*e*) and O—O bond strengths (*D*/kJ mol^{-1}) in the peroxyacetic acid and hydroperoxide molecules calculated by the B3LYP/6-31G(d,p) method

Compound	*q*			*D*(O—O)
	O(2)	O(3)	H(9)	
MeC(O)OOH*	−0.248	−0.306	+0.347	202.3
CF_3OOH[15]	−0.304	−0.295	+0.350	215.0
MeOOH[15]	−0.297	−0.329	+0.332	190.6
Me_3COOH[15]	−0.322	−0.328	+0.331	188.0

* This work.

Table 8. Acidic properties of compounds of general formula RO_xH (calculated by the B3LYP/6-31G(d,p) method)

Compound	q^a/e		Gas-phase acidity[b] /kJ mol^{-1}	pK_a[c] (H_2O, 25 °C)
	O	H		
MeOH	−0.532	+0.306	1700.0	15.5
MeOOH	−0.329	+0.332	1670.8	11.2
MeOOOH	−0.297	+0.336	—	9—10
MeC(O)OOH	−0.306	+0.347	1603.4	8.2
MeC(O)OOOH	−0.273	+0.350	—	—
MeC(O)OH	−0.474	+0.322	1547.2	4.76

[a] Effective atomic charge.
[b] Difference $E_{tot}(RO_x^-) - E_{tot}(RO_xH)$.
[c] Data taken from Refs. 23 and 24.

Alkene epoxidation. The high strength of the peroxide bond precludes homolytic decomposition of PAA, while the IHB favors rearrangement of AcOOH into acetic acid and transfer of the peroxide O atom to the oxidation substrate. In particular, this is the case of the Prilezhaev reaction (alkene epoxidation by peroxy acids). It is assumed that the process involves the formation of a *spiro*-type transition state[25,26] (Scheme 1).

Scheme 1

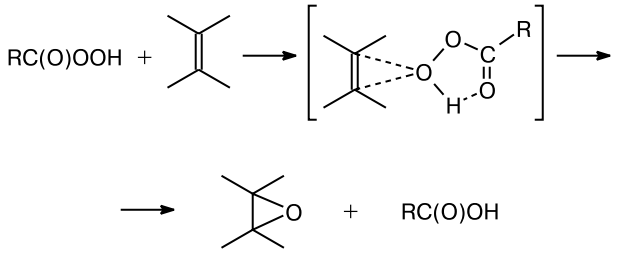

The 1,3-dipolar mechanism of formation of α-oxides[27] (Scheme 2) is also considered, which involves transfer of a proton from the peroxide oxygen atom to the carbonyl O atom and intermediate formation of α-hydroxycarbonyl oxide.

Scheme 2

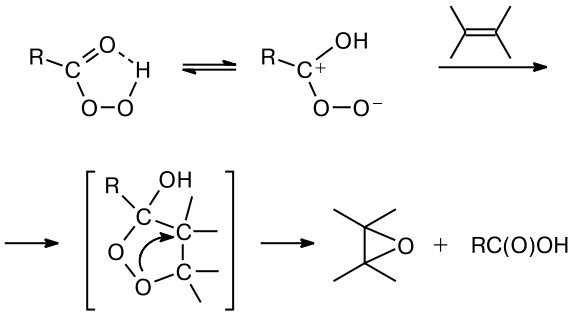

Both reaction mechanisms were quantum-chemically simulated in the B3LYP/6-311++G(d,p) approximation. We studied the possibility of formation of the *syn*- and *anti*-isomers of α-hydroxycarbonyl oxide (PAA can be treated as precursor of this compound,[27] see Scheme 3).

The *syn*-structure was found to be unstable. It does not correspond to the stationary point on the potential energy surface (PES); this means that *syn*-carbonyloxide undergoes spontaneous isomerization into PAA. The *anti*-isomer does correspond to a minimum on the PES but its energy is 185.5 kJ mol^{-1} higher than that of AcOOH. Since the activation energy of alkene epoxidation is much lower than this value, the probability for the *anti*-isomer of α-hydroxycarbonyl oxide to be formed in the reaction under study is negligible. Thus, the 1,3-dipolar mechanism contradicts experimental observations.

Scheme 3

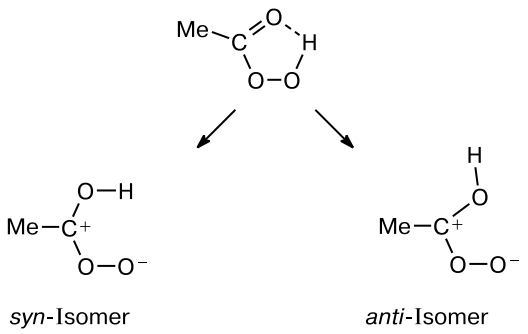

An alternative to this mechanism is provided by the Bartlett mechanism,[25] which was studied taking the reactions of AcOOH with ethylene and cyclohexene as examples. The energies of all reactants and transition states (TS) are listed in Table 9. The geometry of the activated complex is shown in Fig. 5. The transition state is characterized by appreciable lengthening of the peroxide bond. The distance between the carbonyl O atom and the H atom is shorter than in the starting AcOOH molecule but the O—H bond is still to be formed. The O atom of the reaction center is nearly equidistant from carbon atoms of the C=C bond. The plane of the carboperoxyl fragment is perpendicular to the plane of the alkene multiple bond, while the peroxide group and the attacked carbon—carbon bond can be treated as lying in virtually the same plane.

The transition states were characterized by the only imaginary vibrational frequency. The thermal effects of the reactions (ΔH°_{298}) were calculated with inclusion of zero-point vibrational energy correction and reduced to 298 K by calculating the temperature correction, $H^\circ_{298} - H^\circ_0$. The thermal effects of the reactions of both

Table 9. Energy characteristics of reactants and transition states (TS) of alkene epoxidation by peroxyacetic acid

Compopund	E_{tot} /hartree	ZPE[a]	H°_{298} /hartree	S°_{298}[b]	$\Delta_f H^\circ_{298}$[a,c]
AcOOH	−304.312075	169.7	−304.240859	314.8	−353.2
AcOH	−229.164827	161.5	−229.097782	288.1	−432.2
C_2H_4	−78.615539	133.3	−78.560773	218.9	52.3
C_2H_4O	−153.836095	149.9	−153.774901	242.5	−52.7
TS(C_2H_4)	−382.900242	304.6	−382.774316	399.8	—
C_6H_{10}	−234.713213	382.4	−234.561101	303.2	−4.6
$C_6H_{10}O$	−309.937358	396.4	−309.779428	321.9	−125.5
TS(C_6H_{10})	−539.005708	551.3	−538.782582	471.1	—

[a] In kJ mol^{-1}.
[b] In J mol^{-1} K^{-1}.
[c] Data taken from Ref. 17.

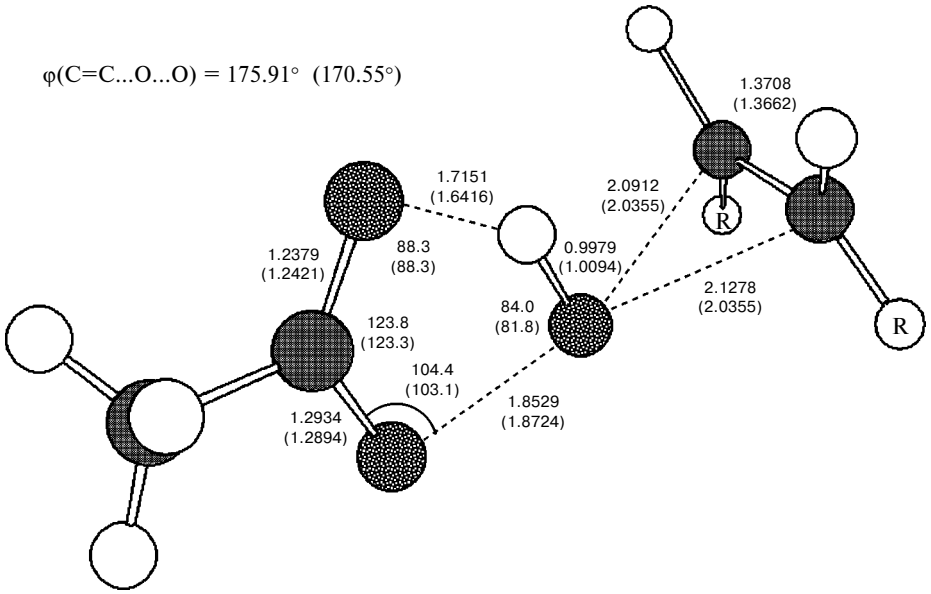

Fig. 5. Transition state of the reaction of cyclohexene (RR = $-(CH_2)_4-$) epoxidation by peroxyacetic acid. The interatomic distances are given in Å and the angles are given in degrees. Figures in parentheses are the corresponding values for the transition state of the reaction of peroxyacetic acid with ethylene (R = H). Calculated by the B3LYP/6-311++G(d,p) method.

olefins are in good agreement with the ΔH° values obtained from calculations of the enthalpies of formation of the reactants[17] and the $\Delta_f H^\circ$(AcOOH) values (see above).

Reaction	ΔH°_{298}/kJ mol^{-1}	
	calculated	Ref. 17
$AcOOH + C_2H_4 \rightarrow AcOH + C_2H_4O$	−186.5	−184.0
$AcOOH + C_6H_{10} \rightarrow AcOH + C_6H_{10}O$	−197.6	−199.9

The activation energy for the reaction of PAA with ethylene is 71.7 kJ mol^{-1}. The activation energy of cyclohexene oxidation is much lower (50.9 kJ mol^{-1}). Our results are in good agreement with the experimental[28,29] values of activation parameters of the reactions of AcOOH with cyclohexene in different solvents (the range of changes in the activation energy is 35.6—75.8 kJ mol^{-1}, pre-exponential factors lg$A$ — 3.88—9.29). The activation energy of the reaction in toluene (the solvent of the lowest polarity) is 51.0 kJ mol^{-1}, which coincides with the calculated value. Small lg$A$ values are also consistent with the entropy of activation ($\Delta S^{\neq}$); according to calculations, $\Delta S^{\neq} = -134.0$ (C_2H_4) and −146.9 J mol^{-1} K^{-1} (cyclohexene). The reaction in toluene is characterized by $\Delta S^{\neq} = -132.1$ J mol^{-1} K^{-1}.[28]

Thus, good agreement between the results of calculations and the experimental data unambiguously supports the Bartlett mechanism.[25,26]

In this work we determined the gas-phase molecular structures of PAA, its dimers, and the complex of AcOOH with water. It was shown that PAA molecules most probably exist in the gas phase and in solution in the monomeric form with intramolecular hydrogen bond, whereas in the solid state the most stable is the dimer with two intermolecular hydrogen bonds, in which the carbonyl O atom acts as the electron density donor. The conformational mobility of the PAA molecule was studied and three types of nonvalent interactions responsible for peculiar features of conformational behavior of this molecule were characterized. These are the intramolecular hydrogen bond, the anomeric effect (stabilization due to the interaction of the LEPs of the peroxide O atoms with the orbitals of adjacent polar bonds), and stabilization of the carboperoxyl fragment. The vibrational spectrum of PAA was calculated (the characteristic bands are those of the O—H, C=O, and O—O stretching vibrations and of the deformation vibrations of the COO, OOH, and carboxyl fragments of the molecule). Using the isodesmic approach and G2 computational procedure, the enthalpies of formation of AcOOH and the acetoxy and acetylperoxy radicals were calculated. High strengths of the O—O and O—H bonds make radical processes involving PAA less probable. Possible mechanisms of alkene epoxidation were analyzed using the results obtained in this work. Transition states of the reactions of AcOOH with ethylene and cyclohexene were located; the energy characteristics of the reactions were found to be in good agreement with the experimental data.

References

1. V. L. Antonovsky, *Organicheskie perekisnye initsiatory* [*Organic Peroxide Initiators*], Khimiya, Moscow, 1972, 448 pp. (in Russian).

2. D. Swern, in *Organic Peroxides*, Ed. D. Swern, Wiley-Interscience, New York, 1970, **1**, 313.
3. V. L. Antonovsky, in *Vestnik Nizhegorodskogo gos. un-ta im. N. I. Lobachevskogo* [*Bull. N. I. Lobachevky Nizhnii Novgorod State Univ.*], Ed. V. A. Dodonov, Izd-vo NNGU, Nizhnii Novgorod, 1996, 3 (in Russian).
4. M. W. Schmidt, K. K. Baldridge, J. A. Boats, S. T. Elbert, M. S. Gordon, J. H. Jensen, S. Koseki, N. Matsunaga, K. A. Nguen, S. J. Su, T. L. Windus, M. Dupuis, and J. A. Montgomery, *J. Comput. Chem.*, 1993, **14**, 1347.
5. M. J. Frisch, G. W. Trucks, H. B. Schlegel, G. E. Scuseria, M. A. Robb, J. R. Cheeseman, V. G. Zakrzewski, J. A. Montgomery, R. E. Stratmann, J. C. Burant, S. Dapprich, J. Millam, M. A. D. Daniels, K. N. Kudin, M. C. Strain, O. Farkas, J. Tomasi, V. Barone, M. Cossi, R. Cammi, B. Mennucci, C. Pomelli, C. Adamo, S. Clifford, J. Ochterski, G. A. Petersson, P. Y. Ayala, Q. Cui, K. Morokuma, D. K. Malick, A. D. Rabuck, K. Raghavachari, J. B. Foresman, J. Cioslowski, J. V. Ortiz, B. B. Stefanov, G. Liu, A. Liashenko, P. Piskorz, I. Komaromi, R. Gomperts, R. L. Martin, D. J. Fox, T. Keith, M. A. Al-Laham, C. Y. Peng, A. Nanayakkara, C. Gonsalez, M. Challacombe, P. M. W. Gill, B. G. Johnson, W. Chen, M. W. Wong, J. L. Andres, M. Head-Gordon, E. S. Replogle, and J. A. Pople, *Gaussian 98 (Revision A.7)*, Gaussian, Inc., Pittsburgh (PA), 1998.
6. A. D. Becke, *J. Chem. Phys.*, 1993, **98**, 5648.
7. A. P. Scott and L. Radom, *J. Phys. Chem.*, 1996, **100**, 16502.
8. A. E. Reed, L. A. Curtiss, and F. Weinhold, *Chem. Rev.*, 1988, **88**, 899.
9. W. J. Hehre, L. Radom, P. v. R. Schleyer, and J. A. Pople, *Ab Initio Molecular Orbital Theory*, Wiley, New York—Chichester—Brisbane, 1986.
10. L. A. Curtiss, K. Raghavachari, G. W. Trucks, and J. A. Pople, *J. Chem. Phys.*, 1991, **94**, 7221.
11. L. A. Curtiss, K. Raghavachari, and J. A. Pople, *J. Chem. Phys.*, 1993, **98**, 1293.
12. S. L. Khursan and V. L. Antonovsky, *Dokl. Akad. Nauk*, 2002, **382**, 657 [*Dokl. Chem.*, 2002 (Engl. Transl.)].
13. D. Swern, L. P. Witnauer, C. R. Eddy, and W. E. Parker, *J. Am. Chem. Soc.*, 1955, **77**, 5537.
14. G. A. Pitsevich, Diss. kand. fiz.-mat. nauk [Ph.D. Thesis (Phys./Math.)], Belarus State University, Minsk, 1985 (in Russian).
15. S. L. Khursan and V. L. Antonovsky, *Izv. Akad. Nauk*, *Ser. Khim.*, 2003, 1241 [*Russ. Chem. Bull.*, *Int. Ed.*, 2003, **52**, 1312].
16. V. L. Antonovsky and M. M. Buzlanova, *Analiticheskaya khimiya organicheskikh peroksidnykh soedinenii* [*Analytical Chemistry of Organic Peroxides*], Khimiya, Moscow, 1978, 308 pp. (in Russian).
17. W. G. Mallard and P. J. Lindstrom, *NIST Chemistry WebBook*, *NIST Standard Reference Database Number 69*, National Institute of Standards and Technology, Gaithersburg, February 2000.
18. S. S. Levush, Z. P. Prisyazhnyuk, and A. M. Koval´skaya, *Kinet. Katal.*, 1983, **24**, 1294 [*Kinet. Catal.*, 1983, **24** (Engl. Transl.)].
19. S. S. Levush, Z. P. Prisyazhnyuk, and A. M. Koval´skaya, *Ukr. Khim. Zh.* (*Rus. Ed.*) [*Ukr. Chem. J.*], 1983, **49**, 833 (in Russian).
20. V. L. Antonovsky and K. V. Bozhenko, *Dokl. Akad. Nauk*, 1995, **343**, 337 [*Dokl. Chem.*, 1995 (Engl. Transl.)].
21. V. L. Antonovsky, K. V. Bozhenko, and D. Kh. Kitaeva, *Izv. Akad. Nauk, Ser. Khim.*, 1998, 600 [*Russ. Chem. Bull.*, 1998, **47**, 578 (Engl. Transl.)].
22. A. J. Kirby, *The Anomeric Effect and Related Stereoelectronic Effects at Oxygen*, Springer-Verlag, Berlin—Heidelberg—New York, 1983.
23. D. J. McKay and J. S. Wright, *J. Am. Chem. Soc.*, 1998, **120**, 1003.
24. V. V. Shereshovets, S. L. Khursan, V. D. Komissarov, and G. A. Tolstikov, *Usp. Khim.*, 2001, **70**, 123 [*Russ. Chem. Rev.*, 2001, **70** (Engl. Transl.)].
25. P. D. Bartlett, *Rec. Chem. Progr.*, 1950, **11**, 47.
26. B. M. Lynch and K. H. Pausacker, *J. Chem. Soc.*, 1955, 1525.
27. H. Kwart and D. M. Hoffman, *J. Org. Chem.*, 1966, **31**, 419.
28. Ya. M. Vasyutyn, G. G. Midyana, R. G. Makitra, Ya. N. Pirig, and V. I. Timokhin, *Dokl. Akad. Nauk Ukr. SSR*, *Ser. B* [*Dokl. Acad. Sci. Ukr. SSR*, *Ser. B*], 1985, 39 (in Russian).
29. V. G. Dryuk, M. S. Malinovskii, S. P. Shamrovskaya, S. A. Vasil´chenko, and S. A. Maslov, *Zh. Org. Khim.*, 1973, **9**, 1228 [*J. Org. Chem. USSR*, 1973, **9** (Engl. Transl.)].

Received November 1, 2002;
in revised form May 26, 2003